Supporting Information

A. Chemicals and Synthesis
All oligonucleotides were purchased from Integrated DNA Technologies (IDT) with standard desalting and used without further purification. Silver nitrate (99.9999%) and sodium borohydride (99%) were used as received from Sigma Aldrich. All solutions were prepared using nuclease-free, deionized water (IDT), in fresh plasticware, using fresh gloves. Unless otherwise stated in the article text, Ag:DNA and Ag:RNA solutions were prepared by mixing 200 μM DNA (RNA) strands with 160mM ammonium acetate and 20mM $AgNO_3$, followed by reduction with $NaBH_4$, with final concentrations of 80μM strands, 10mM ammonium acetate, 880μM $AgNO_3$ and 488μM $NaBH_4$, at pH 6.8.

RNA and DNA oligonucleotides studied:

RNA $r(U_2C_3)$, $r(UC_4)$, $r(C_5)$. $r(U_2G_2U)$, $r(UG_3U)$, $r(UG_4U)$, $r(UG_5U)$.
$r(A_6)$, $r(C_6)$, $r(G_6)$, $r(UG_6U)$, $r(U_6)$. $r(A_{11})$, $r(C_{11})$, $r(UG_{11}U)$, $r(U_{11})$.

DNA $d(T_2C_3)$, $d(TC_4)$, $d(C_5)$. $d(TG_3T)$, $d(TG_4T)$, $d(TG_5T)$. $d(C_8)$, $d(TG_8T)$. $d(C_7)$, $d(C_{10})$.
$d(A_6)$, $d(C_6)$, $d(TG_6T)$, $d(T_6)$. $d(A_9)$, $d(C_9)$, $d(TG_9T)$, $d(T_9)$. $d(A_{11})$, $d(C_{11})$, $d(G_{11})$, $d(TG_{11}T)$, $d(T_{11})$.

d(TTTATTTATTTATTT),d(ATTTAATTATATATA),d(AATAATAATAATA),
d(ATATTATTTATTTTA),d(TAAATTAATATATAT),d(AAATAATTAAATA),
d(ATATTATTATTATAT),d(TAAATTAAAATATAT),d(AAAAATAAAAATA).
These mixed (A,T) strands were designed to have mfold melting temperatures < 3ºC for all loops, well below the measurement temperature of 22ºC.

B. Experimental Procedures for Mass Spectrometry: Spectra were measured using a Micromass QTOF2 mass spectrometer in negative ion mode with an electrospray ionization source. Samples were run at 10μL/min flow rate, 2.5 kV capillary voltage and 45 V cone voltage.

C. Solution conditions used to test the generality of the C,G vs A,T/U dichotomy:
In addition to the solution conditions described in the main text, we measured fluorescence spectra of Ag:RNA and Ag:DNA solutions prepared at

A) strand concentrations of 10, 20, 30, and 50 μM, at 11 Ag/strand;
B) salt concentrations of 2.5, 5 and 10 mM Mg^{++} (magnesium acetate) and 25, 50 and 100 mM Na^{+} (sodium acetate), at 80 μM strand concentration and 11 Ag/strand, and
C) silver/strand ratios of 4:1 and 20:1, at 80 μM strand concentration.

D. Gel Electrophoresis: RNA structures, described elsewhere [22], were analyzed on a 7% (37.5:1) non-denaturing polyacrylamide native gel containing 2 mM $Mg(OAc)_2$ and 50 mM KCl. Gels were run at 4ºC with running buffer (89 mM Tris-borate, pH 8.3/ 2mM $Mg(OAc)_2$). An equal volume of loading buffer (the running buffer with 0.01% bromphenol blue, 0.01% xylene cyanol, 50% glycerol) was added to each sample before loading on native gel.

E. Fluorescence measurements: Excitation was by a Xenon lamp, passed through a monochromator with 4 nm resolution. To remove instrumental effects, all spectra have been normalized by the monochromator throughput of the excitation light. Emission spectra were collected with a thermoelectrically-cooled array detector (Ocean Optics QE-65000).

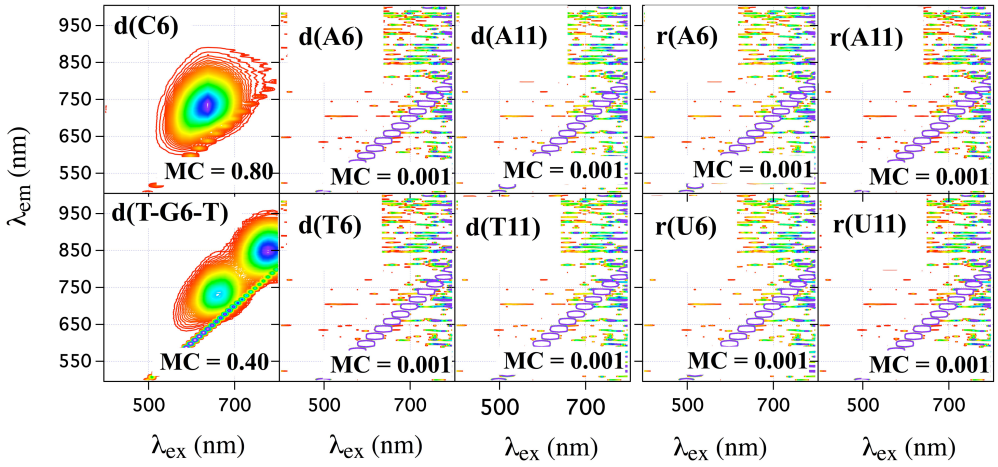

Figure S1. Fluorescence contour maps of Ag:DNA and Ag:RNA solutions display the absence of fluorescence from Ag:poly(dA),Ag:poly(dT), Ag:poly(rA) and Ag:poly(rU) solutions for excitation across the 360nm-850 nm range. *The signal is indistinguishable from detector noise.* Left column: For comparison, fluorescence contour maps of Ag:d(C_6) and Ag:d(TG_6T) solutions are shown. In all cases, strand concentrations were 80 μM and synthesis was at 11 Ag/strand. All fluorescence spectra were measured 25 hours after reduction. Purple corresponds to the maximum contour (MC) level, indicated on each plot in identical, arbitrary intensity units.

These results are representative: across all strand concentrations, silver concentrations and salt concentrations, there was no detectable fluorescence from Ag:poly(dA),Ag:poly(dT), Ag:poly(rA) and Ag:poly(rU) solutions, for excitation from 360 nm – 850 nm.

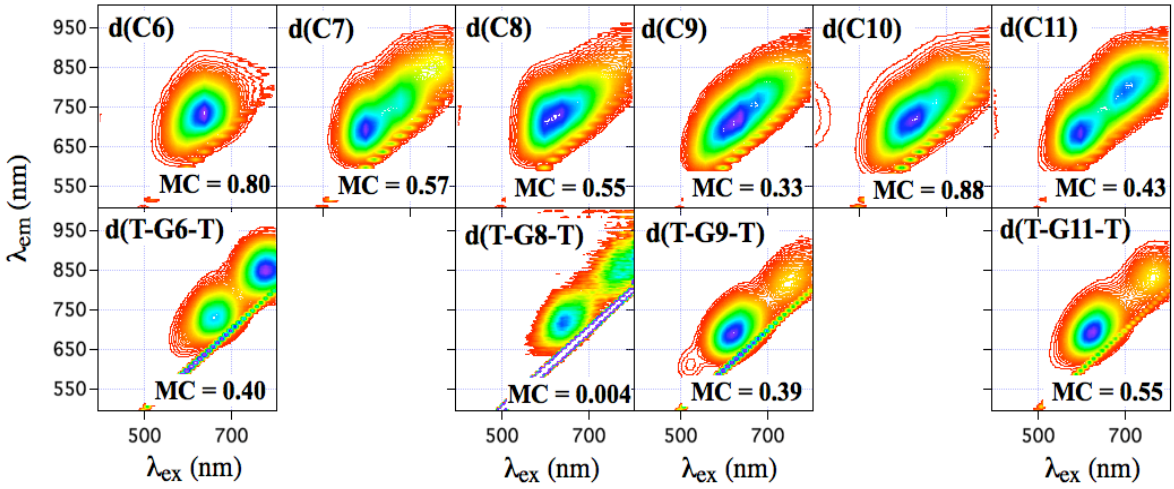

Figure S2. Fluorescence contour maps of Ag:DNA solutions across a wider range of strand lengths, for excitation across the 360nm-850 nm range. Strands concentrations were 80 μM and synthesis was at 11 Ag/strand. The data show only weak variation in peak fluorescence intensity (with the exception of d(TG_8T)), but considerable variation in spectral distribution.

Figure S3.

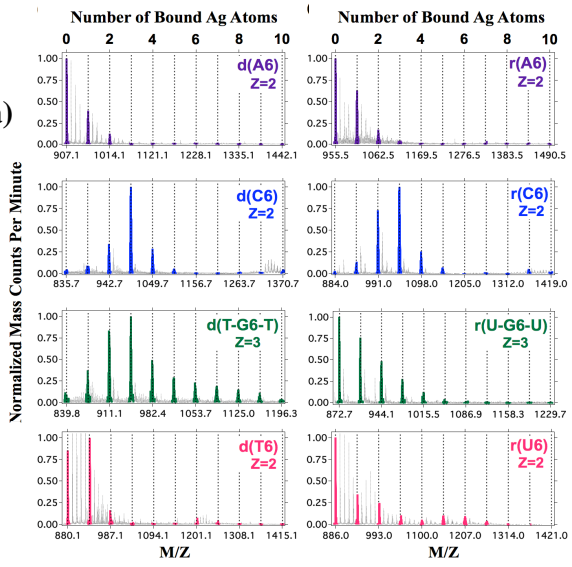

(a) Mass Spectra show silver binding to DNA (left panels) and RNA (right panels) strands with 6-mer homopolymer runs of all base types.

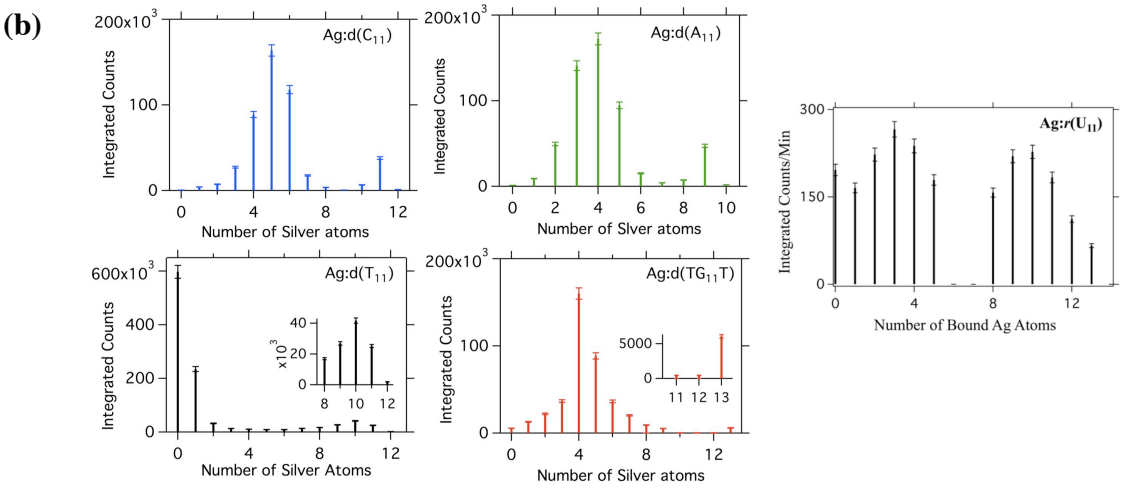

(b) Mass abundances versus number of silver atoms attached to the strand for Ag:DNA solutions with 11-mer homopolymer runs and for Ag:r(U_{11}), 25 hours after synthesis (80 µM strands and 11 Ag/strand). The vertical bars are the integrated counts for the various silver products**. For simplicity, only the signal for the sodium-free species is shown.
All strand types exhibit enhanced mass counts at silver atom numbers N~10.
(We note that electrospray ionization rates depend on strand composition. Thus the count rate from mass spectra cannot be used to estimate comparative yields between different strands).

** To extract the integrated counts for the various silver products in Fig. S3(b), the raw data were integrated across a window of fixed width in M/Z for each sodium-free silver-strand product, for the charge state corresponding to the highest count rate. Different charge states, and different sodium adducts, resulted in similar relative count rates for the different silver products. In every case we verified by direct inspection that the signal present displayed the expected isotope peak periodicity for that Z. For the rare cases in which silver products from a different Z produced overlapping signal, we integrated the signal for the charge state of the next highest count rate and normalized this value using neighboring silver atom peaks.

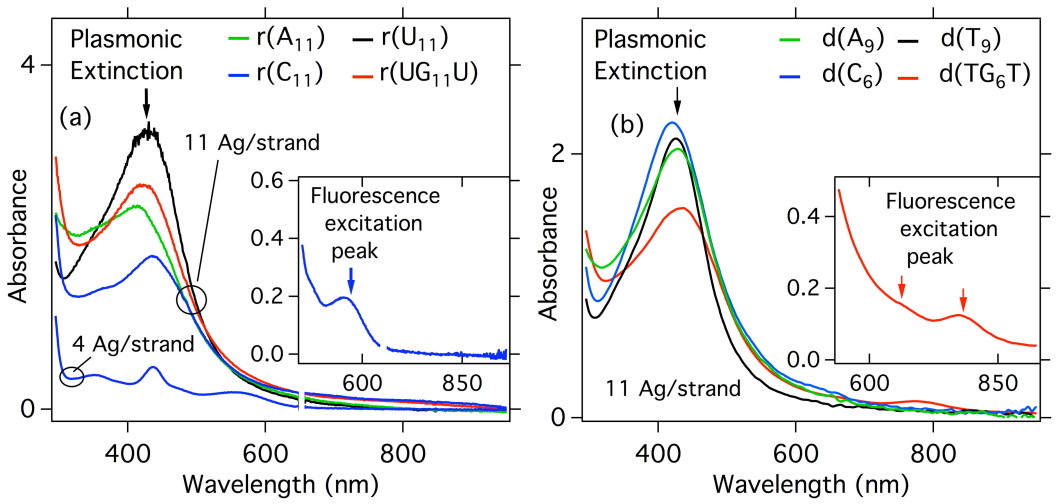

Figure S4. Representative absorbance spectra for (a) Ag:RNA solutions and (b) Ag:DNA solutions. All exhibit high extinction in the wavelength range expected for plasmonic absorption and scattering by silver nanoparticles, ~10-100 nm in diameter (~400-500 nm) [25], though other excitation processes may be responsible. Such nanoparticles have peak cross-sections a factor of ~10^5-10^6 larger than reported for Ag:DNA fluorophores [8], and thus, if present, they would dominate extinction even if their concentration were much lower than that of the silver nanoclusters.

We found that excitation across the plasmonic extinction range produced no fluorescence from any of the many solutions studied, regardless of strand length, strand type (RNA or DNA), or silver content, with the sole exception of the Ag:d(C_{11}) solution at 4 Ag/strand, which exhibited a fluorescence excitation maximum near 450 nm.

Insets: Absorbance peaks that correspond to excitation of silver cluster fluorescence rise above the broad background for the longest-wavelength emitters. Arrows mark peak fluorescence excitation wavelengths.

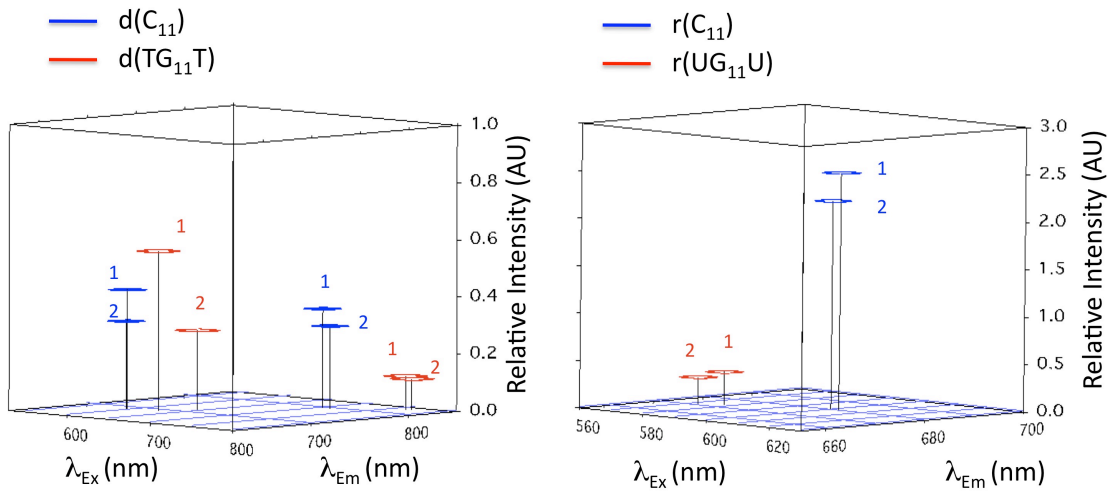

Figure S5. Comparison of the brightness and stability of silver cluster fluorophores stabilized by DNA and RNA strands with homopolymer runs of eleven C and G bases. Vertical axis is emission intensity, in identical arbitrary units for RNA and DNA. Horizontal axes are peak emission and excitation wavelengths. The "drop down" lines from the data points identify their wavelength. Points labeled "1" and "2" were measured at 24 hours and one week after reduction, on aliquots stored at 4 ºC.

Figure S6.

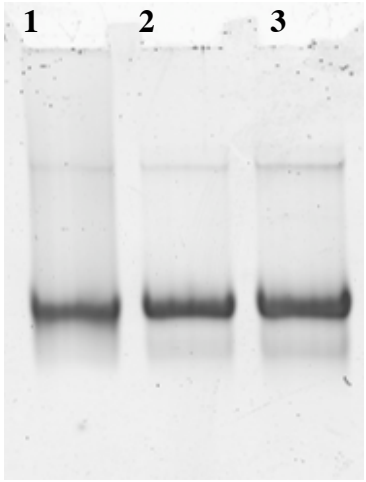

(a) Native PAGE gel of a 312 nucleotide RNA structure described in [22], with and without silver cluster synthesis. Lane 1 (control): RNA only. Lane 2: RNA with $NaBH_4$. Lane 3: RNA 24 hours after silver cluster synthesis. The final concentrations of Ag synthesis reagents in lane 3 were 5μM RNA, 16mM ammonium acetate, 55μM $AgNO_3$ and 28μM $NaBH_4$. All lanes were loaded with the same volume of 5μM RNA; lanes 2 and 3 with equal concentrations of $NaBH_4$. The similarity of the bands in lanes 1 and 3 indicate that the RNA is not damaged under the solution conditions for Ag cluster synthesis. (We thank Kirill Afonin for this image).